

2

Mechanical Properties and Microstructure of Centrifugally Cast Alloy 718

D. J. MICHEL AND H. H. SMITH

*Thermostructural Materials Branch
Material Science and Technology Division*

November 14, 1984

AD-A147 800



NAVAL RESEARCH LABORATORY
Washington, D.C.

DTIC
SELECTE
NOV 27 1984
S A D

DTIC FILE COPY

Approved for public release; distribution unlimited.

84 11 26 205

REPORT DOCUMENTATION PAGE				
1a REPORT SECURITY CLASSIFICATION UNCLASSIFIED		1b RESTRICTIVE MARKINGS		
2a SECURITY CLASSIFICATION AUTHORITY		3 DISTRIBUTION AVAILABILITY OF REPORT		
2b DECLASSIFICATION/DOWNGRADING SCHEDULE		Approved for public release; distribution unlimited.		
4 PERFORMING ORGANIZATION REPORT NUMBER(S) NRL Memorandum Report 5431		5 MONITORING ORGANIZATION REPORT NUMBER(S)		
6a NAME OF PERFORMING ORGANIZATION Naval Research Laboratory	6b OFFICE SYMBOL (if applicable) Code 6390	7a NAME OF MONITORING ORGANIZATION Naval Air Systems Command		
6c ADDRESS (City, State, and ZIP Code) Washington, DC 20375-5000		7b ADDRESS (City, State, and ZIP Code) Washington, DC 20361		
8a NAME OF FUNDING SPONSORING ORGANIZATION Naval Material Command	8b OFFICE SYMBOL (if applicable) MAT 064	9 PROCUREMENT INSTRUMENT IDENTIFICATION NUMBER		
8c ADDRESS (City, State, and ZIP Code) Washington, DC 20360		10 SOURCE OF FUNDING NUMBERS		
		PROGRAM ELEMENT NO	PROJECT NO	TASK NO.
				WORK UNIT ACCESSION NO DN291-257
11 TITLE (include Security Classification) Mechanical Properties and Microstructure of Centrifugally Cast Alloy 718				
12 PERSONAL AUTHOR(S) Michel, D.J. and Smith, H.H.				
13a TYPE OF REPORT Final	13b TIME COVERED FROM 10/82 TO 5/84	14 DATE OF REPORT (Year, Month, Day) 1984 November 14	15 PAGE COUNT 32	
16 SUPPLEMENTARY NOTATION				
17 COSATI CODES		18 SUBJECT TERMS (Continue on reverse if necessary and identify by block number)		
FIELD	GROUP	SUB-GROUP		
			Tensile strength Fatigue Mechanical properties	
			Creep-rupture strength Crack propagation Elevated temperatures	
19 ABSTRACT (Continue on reverse if necessary and identify by block number) <p>The relationship between the microstructure and mechanical properties of alloy 718 was investigated for two discs centrifugally cast at 50 and 200 rpm and given a duplex age heat treatment. The results of mechanical property tests at temperatures from 426 to 649 °C showed that the tensile yield and ultimate strength levels of both castings were similar. However, the creep-rupture properties were considerably enhanced for the casting produced at 200 rpm. Comparison of the radial and transverse creep properties of each disc indicated that creep life was generally independent of orientation, but ductility was greatest for specimens oriented transverse to the radial direction of the casting. Fatigue crack propagation performance was not greatly influenced by orientation or mold speed parameters and was comparable to wrought Alloy 718 when compared on the basis of stress intensity factor range. The centrifugal casting process was found to produce a homogeneous microstructure free of porosity but with the expected segregation of solute alloying elements to Laves and carbide phases. The effect of the as-cast microstructure on the mechanical behavior and the potential influence of hot isostatic pressing to improve the microstructure are discussed.</p>				
20 DISTRIBUTION AVAILABILITY OF ABSTRACT <input checked="" type="checkbox"/> UNCLASSIFIED UNLIMITED <input type="checkbox"/> SAME AS RPT <input type="checkbox"/> DTIC USERS		21 ABSTRACT SECURITY CLASSIFICATION UNCLASSIFIED		
22a NAME OF RESPONSIBLE INDIVIDUAL D. J. Michel		22b TELEPHONE (include Area Code) (202) 767-2621	22c OFFICE SYMBOL Code 6390	

CONTENTS

INTRODUCTION	1
EXPERIMENTAL PROCEDURES	1
Material and Heat Treatments	1
Specimen Preparation	2
Mechanical Property Evaluations	2
Microscopy and Analysis	4
RESULTS	4
Tensile Test Results	4
Creep-Rupture Test Results	5
Fatigue Crack Propagation Test Results	5
Metallographic Results	5
Fractographic Results	21
DISCUSSION	21
SUMMARY AND CONCLUSIONS	26
ACKNOWLEDGMENTS	27
REFERENCES	28



Administrative stamp with fields for:

- APPROVED
- DATE
- BY
- REMARKS

A-1

MECHANICAL PROPERTIES AND MICROSTRUCTURE OF CENTRIFUGALLY CAST ALLOY 718

INTRODUCTION

Alloy 718 is a complex precipitation hardened, nickel-base alloy widely used for gas turbine engine components. Currently, alloy 718 is employed in the form of highly stressed components produced by forging and machining operations. As such, these components are costly in terms of labor, capital equipment and energy input. However, the mechanical properties of alloy 718 cast to shape by conventional methods is marginal to meet the strength, creep-rupture and fatigue crack propagation requirements for engine components.

The application of advanced casting techniques to improve the properties of cast alloy 718 will permit the production of components cast to near net shape thereby eliminating most machining operations. Previous work has suggested that cast properties can be produced which approach those of forgings when the solidification rates and parameters are controlled to achieve the proper microstructure.

The purpose of this report is to present the results from a study of the properties and microstructure of centrifugally cast alloy 718 produced with two mold speeds. The results show that the fatigue properties of the cast alloys were similar to those of the wrought alloy when compared on the basis of stress intensity factor range. Although the tensile strength of the cast alloy was less than for the wrought alloy, the creep properties of the cast alloy exceed those of the wrought alloy for creep loads determined on the basis of fraction of the tensile yield strength of each product form.

EXPERIMENTAL PROCEDURES

Material and Heat Treatments

The chemical composition of the cast alloy 718 and the heat treatment details are given in Table 1. The castings were produced in the form of flat discs (approximately 2.54 cm thick by 25.4 cm outside diameter by 7.62 cm inside diameter) using two different mold rotation speeds, 50 and 200 rpm. The castings were given the duplex age heat treatment shown in Table 1 to develop the γ'' precipitate microstructure for increased strength. Figure 1 shows a photograph of the cast disc and a prototypic compressor impeller cast by the centrifugal casting process.

Manuscript approved July 9, 1984.

TABLE I

Chemical Composition and Heat Treatment
of Cast Alloy 718

<u>Composition (weight percent)*</u>					
C	0.056	Cr	19.60	Co	0.010
Mn	0.010	Ni	53.40	Fe	Bal
P	0.004	Ti	1.05	Cu	0.010
S	0.004	Al	0.48	B	0.003
Si	0.010	Mo	3.09	Nb/Ta	5.22

*Vendor supplied analysis.

Heat Treatment

<u>Temperature</u>	<u>Time</u>	
718°C (1325°F)	8 Hrs.	Furnace cool at 56°C (100°F) per hr.
621°C (1150°F)	8 Hrs.	to air cool

Specimen Preparation

Specimen blanks were cut from the as received castings either above or below the mid-plane of the discs. Tensile/creep and 0.5T CT (compact tension) fatigue crack propagation specimens were machined from the blanks in accordance with ASTM Standards E8 and E647 [1,2]. The notch in the CT specimens and gage length in the tensile/creep specimens were oriented either in the radial direction or transverse to the radial direction of the castings. All of the CT specimens were precracked in accordance with ASTM Standard E647 [2] such that the final K_{max} during precracking did not exceed the initial K_{max} of the fatigue test.

Mechanical Property Evaluations

The tensile, creep and fatigue tests were conducted at 427, 538 and 649°C (800, 1000 and 1200°F) in air. These temperatures were achieved through resistance heating except for fatigue tests at 427 and 538°C where induction heating was employed. The reported data represent the mechanical properties of the alloy 718 cast at mold speeds of 50 and 200 rpm for radial and transverse specimen orientations.

Tensile tests were conducted using an Instron Tensile Testing Machine. Crosshead speed was maintained at 1.27×10^{-2} cm/min (5×10^{-3} in/min) throughout the test. The calculated values of 0.2% offset tensile yield strength were based on extension derived from motion of the crosshead. This practice was considered satisfactory due to the relatively large extensions and low loads



R-1083

Fig. 1 Centrifugally cast alloy 718 test disc and prototype impeller.

employed for these tests. Reported values of elongation are a result of post test measurements of change in overall specimen length.

Creep tests were performed on lever arm creep frames using specimens which were identical to those used for the tensile tests. Test loads were based on the ratio of the creep stress to the 0.2% offset tensile yield stress as determined specifically for each condition of test temperature, casting speed and material orientation. Creep extension was recorded continuously during the test using a LVDT to measure displacement of the specimen grips. Reported values of elongation are based on change of spacing of prickmarks (25.4 mm, 1 in. initial spacing) on the specimen gauge length after test completion.

Fatigue crack growth tests were performed on an electrohydraulic MTS machine operated in the load control mode. All tests were conducted in air at a load ratio of 0.05 employing a triangular waveform at 0.17 Hz. Crack length was measured using a traveling microscope to follow crack growth on one side of the specimen. The data obtained from the fatigue crack propagation tests were analyzed to yield crack growth rate, da/dN , as a function of the stress intensity factor range, ΔK . Crack growth rates were determined through computer curve fitting of the crack length versus cycle data and differentiation of the resulting fitted curve. The stress intensity factor was derived using the ASTM committee E-24 recommendations for CT specimens of this configuration.

Microscopy and Analysis

Macro and microstructural features of the casting were investigated using conventional optical and electron microscopic techniques. Bulk compositional analyses of unetched, polished samples (sample area of approximately 2.3 mm²) taken along the radial direction of both castings were performed using x-ray fluorescence spectroscopy. The analyses were performed using a Sn target at 0.8 mA and a tube potential of 40 Kv. Compositional values of weight percent were calculated from the comparison of Ti, Cr, Fe, Nb and Mo ratios with respect to Ni between the cast alloy and a highly documented 718 alloy. Optical macrographs were taken to show the dendrite structure for the radial and transverse directions of the castings. The composition and features of the various phases in the microstructure were analyzed using a JSM-35C scanning electron microscope/microprobe in conjunction with a standardless semi-quantitative analysis program. Details of the fracture processes for tensile, creep, and fatigue failure were investigated by fractographic analysis and by use of polished and etched metallographic sections of the crack. The etchants used in this study were an electrolytic etch of H₂SO₄:H₃PO₄:HNO₃ of the volume ratio 47:41:12 and HF:HNO₃:H₂O of the volume ratio 1:2:8.

RESULTS

Tensile Test Results

The tensile yield and ultimate stress levels of the cast alloy 718 were determined at temperatures of 427, 538 and 649°C (800, 1000 and 1200°F) using a strain rate of 7.4×10^{-5} sec⁻¹. The specimens were oriented both

parallel and perpendicular to the radial direction of the cast discs. The tensile properties are summarized in Table 2. The results show that the stress levels of the cast materials from either casting and in either stress direction are similar at each test temperature reflecting little directionality of the cast tensile properties.

Creep-Rupture Test Results

The creep-rupture properties of the cast alloy 718 were determined at temperatures of 427 and 538°C at 100% of the offset yield stress and at 649°C at 85%, 90%, and 100% of the offset yield stress. The results from all creep-rupture tests are summarized in Table 3. The results at 649°C for both mold speeds also are plotted in Figures 2 and 3. Comparison of the figures show that the creep life of the 200 rpm casting was enhanced over that of the 50 rpm casting. It can be seen that in creep, the cast material exhibits increased ductility when stressed perpendicular to the radial direction of the casting even though creep life was generally independent of orientation. Comparison of these results with test results from wrought alloy 718 plate material, Figure 4, shows that, at similar fractions of the yield stress level at 649°C, the creep-rupture lives and ductility of the cast alloys were significantly greater than for the wrought alloy; however, note the higher absolute value of the stress for the wrought alloy.

Fatigue Crack Propagation Test Results

The fatigue crack propagation performance of the cast alloy 718 was investigated at temperatures of 427, 538 and 649°C. The results are shown in Figures 5 through 8. Comparison of Figures 5 and 6, for specimens oriented such that the crack propagation path was perpendicular to the cast disc radial direction, shows that the crack propagation rates of the two castings were similar at 427 and 538°C. At 649°C, the crack propagation rate for material cast with a 200 rpm mold speed was considerably lower than for the material cast with a 50 rpm mold speed. However, for specimens oriented such that the crack path was parallel to the cast disc radial direction, Figures 7 and 8 show that the crack propagation rates at all three temperatures were similar for both cast disc materials. Comparison of the cast alloy crack propagation results with those for wrought alloy 718 [3,4] shows that crack propagation rates at 427°C are nearly identical while the rates at 649°C are higher for the wrought alloy.

Metallographic Results

Optical and electron methods were used to examine the microstructure of the cast alloy 718. The compositional homogeneity of the casting was investigated by analysis of six areas from the inner radius to the outer radius along the radial plane of each casting. The results of the x-ray fluorescence spectroscopy are summarized in Table 4. Comparison of these results with the chemical analysis in Table 1 shows good agreement although the percentage of titanium is slightly low for the x-ray fluorescence results. (The actual percentage of titanium may be somewhat higher because a Sn target was used which increases the accuracy of the analysis of molybdenum and niobium, but decreases the accuracy of the analysis for titanium.) The amount of these elements is important because they are the

TABLE 2

Cast High Strength Alloy 718 Tensile Properties

<u>Specimen No.*</u>	<u>Test Temp.</u> <u>°C</u>	<u>Yield Stress</u> <u>(0.2% offset, Ksi)</u>	<u>Ultimate</u> <u>Stress</u> <u>Ksi</u>	<u>Elongation</u> <u>(%)</u>
E3A1	427	86.4	101.8	5.9
E3A3	427	88.3	99.3	4.6
E3A5	427	90.8	112.0	10.4
E3A2	649	84.7	94.5	3.0
E3A4	649	84.9	94.1	3.4
E3A6	649	89.7	100.6	5.1
E3B4	427	92.9	111.6	6.6
E3B1	538	88.5	101.1	3.6
E3B5	649	87.2	101.0	6.6
G3A1	427	88.8	111.6	11.6
G3A4	427	88.8	110.0	10.7
G3A2	538	85.3	106.4	7.2
G3A5	538	89.6	110.0	8.4
G3A3	649	85.8	103.0	6.9
G3A6	649	88.8	102.3	6.4
G3B4	427	92.1	112.0	7.1
G3B1	538	90.4	112.9	9.4
G3B5	649	87.2	99.8	4.2

*E = 50 rpm mold speed.

G = 200 rpm mold speed.

A = Specimen stress axis perpendicular to cast disc radial direction.

B = Specimen stress axis parallel to cast disc radial direction.

TABLE 3

Cast High Strength Alloy 718 Creep Properties

<u>Specimen No.*</u>	<u>Test Temp. °C</u>	<u>Creep Stress (Fract. 0.2% yield)</u>	<u>Rupture Life (hrs)</u>	<u>Rupture Strain (max. %)</u>
E3A10	649	1.00	4	4.3
E3A12	649	1.00	4	4.4
E3A07	649	0.85	147	6.9
E3B06	649	1.00	10	4.1
E3B12	649	0.90	40	3.1
E3B10	649	0.85	145	4.3
E3B02	538	1.00	1000**	
E3B03	427	1.00	1000**	
G3A09	649	1.00	11	7.1
G3A12	649	0.85	250	8.3
G3B06	649	1.00	1	2.7
G3B12	649	0.85	235	4.1
G3B02	538	1.00	1000**	
G3B03	427	1.00	1000**	

*E = 50 rpm mold speed.

G = 200 rpm mold speed.

A = Specimen stress axis perpendicular to cast disc radial direction.

B = Specimen stress axis parallel to cast disc radial direction.

**Test terminated at 1000 hours without specimen failure.

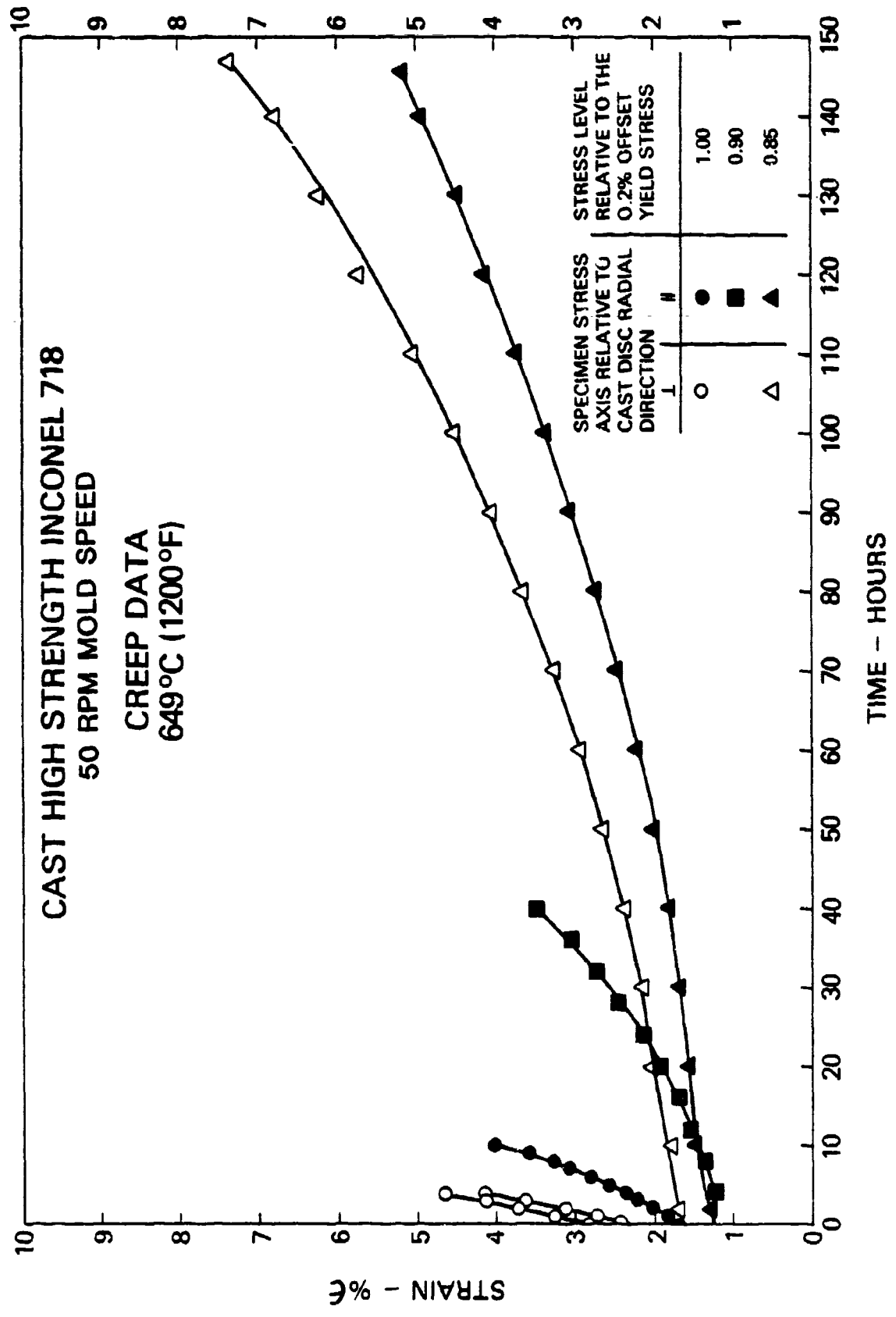


Fig. 2 Strain versus time for cast alloy 718 (50 rpm mold speed) tested at 649°C.

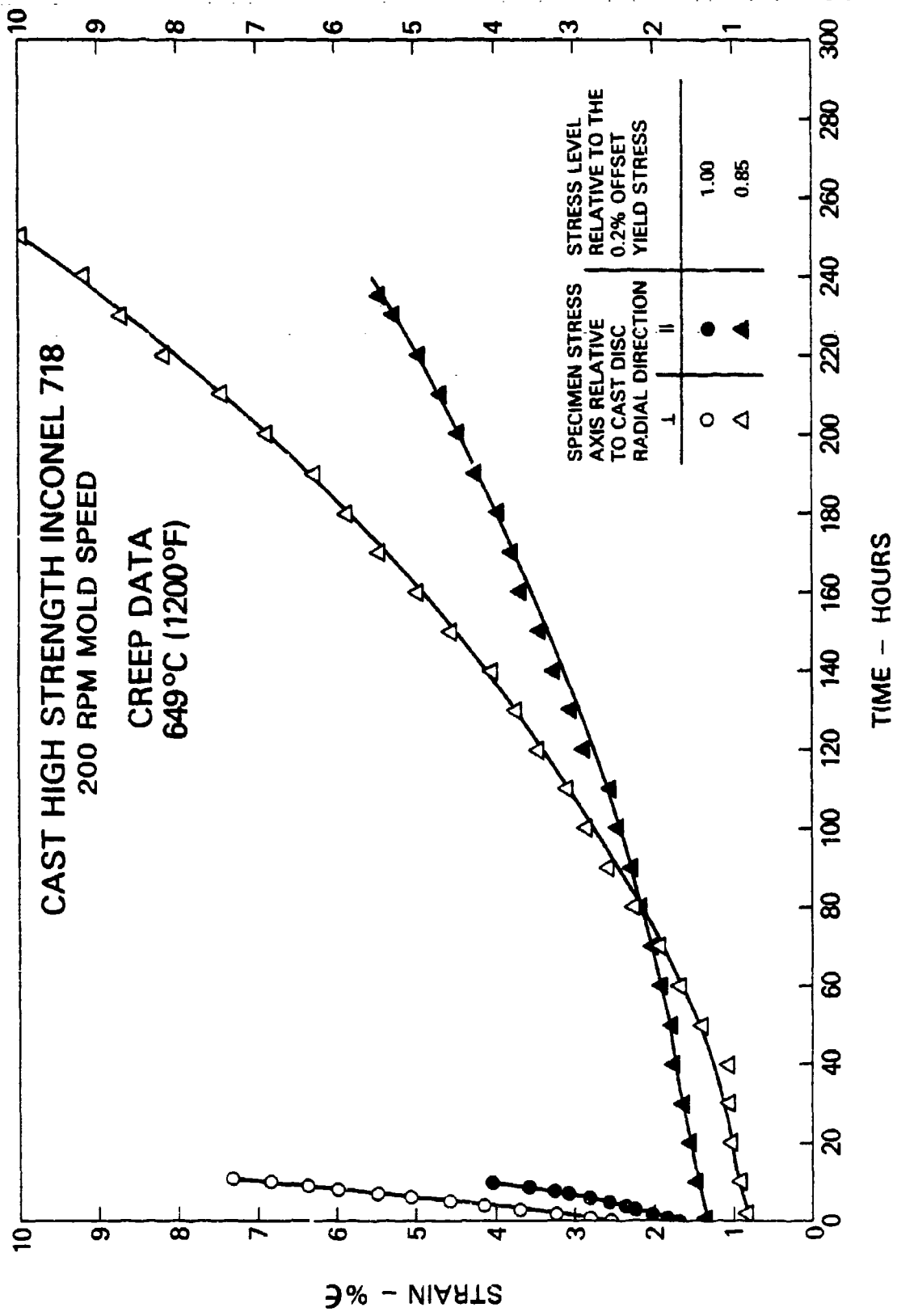


Fig. 3 Strain versus time for cast alloy 718 (200 rpm mold speed) tested at 649°C.

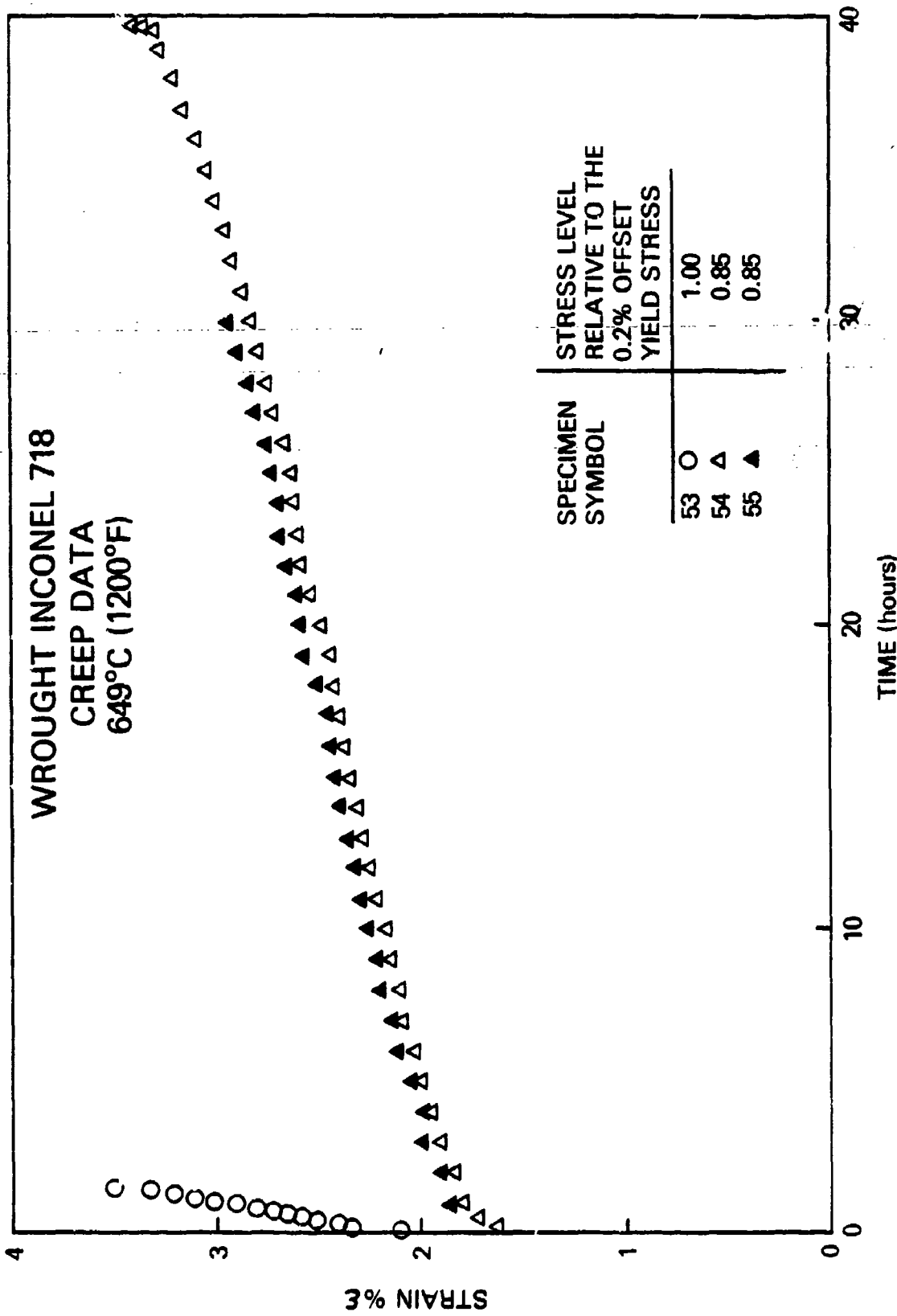


Fig. 4 Strain versus time for wrought alloy 718 tested at 649°C.

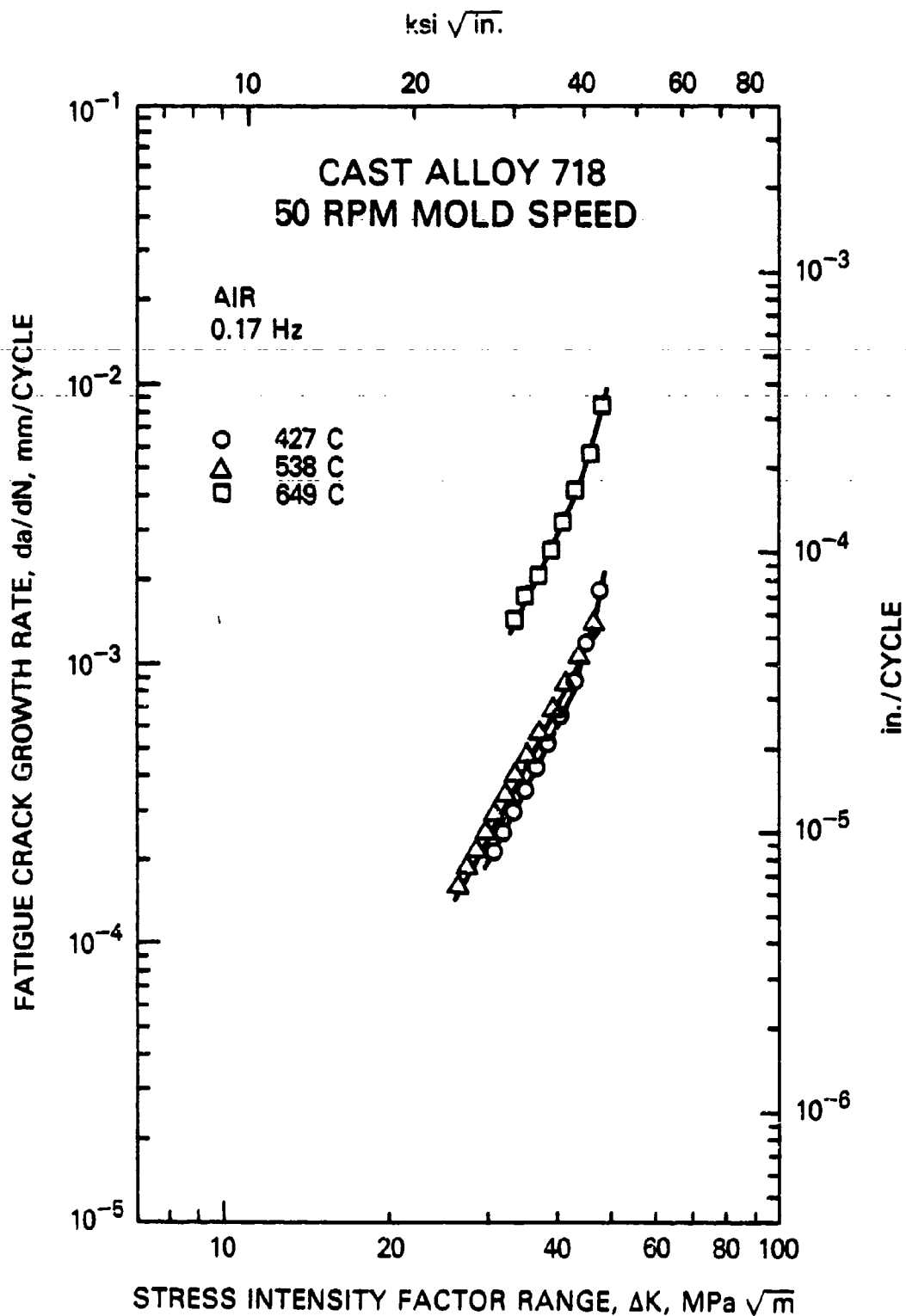


Fig. 5 Fatigue crack propagation performance of alloy 718 (50 rpm mold speed) in air at 0.17 Hz and at 427, 538 and 649°C. Notch orientation of the specimens was perpendicular to the cast disc radial direction.

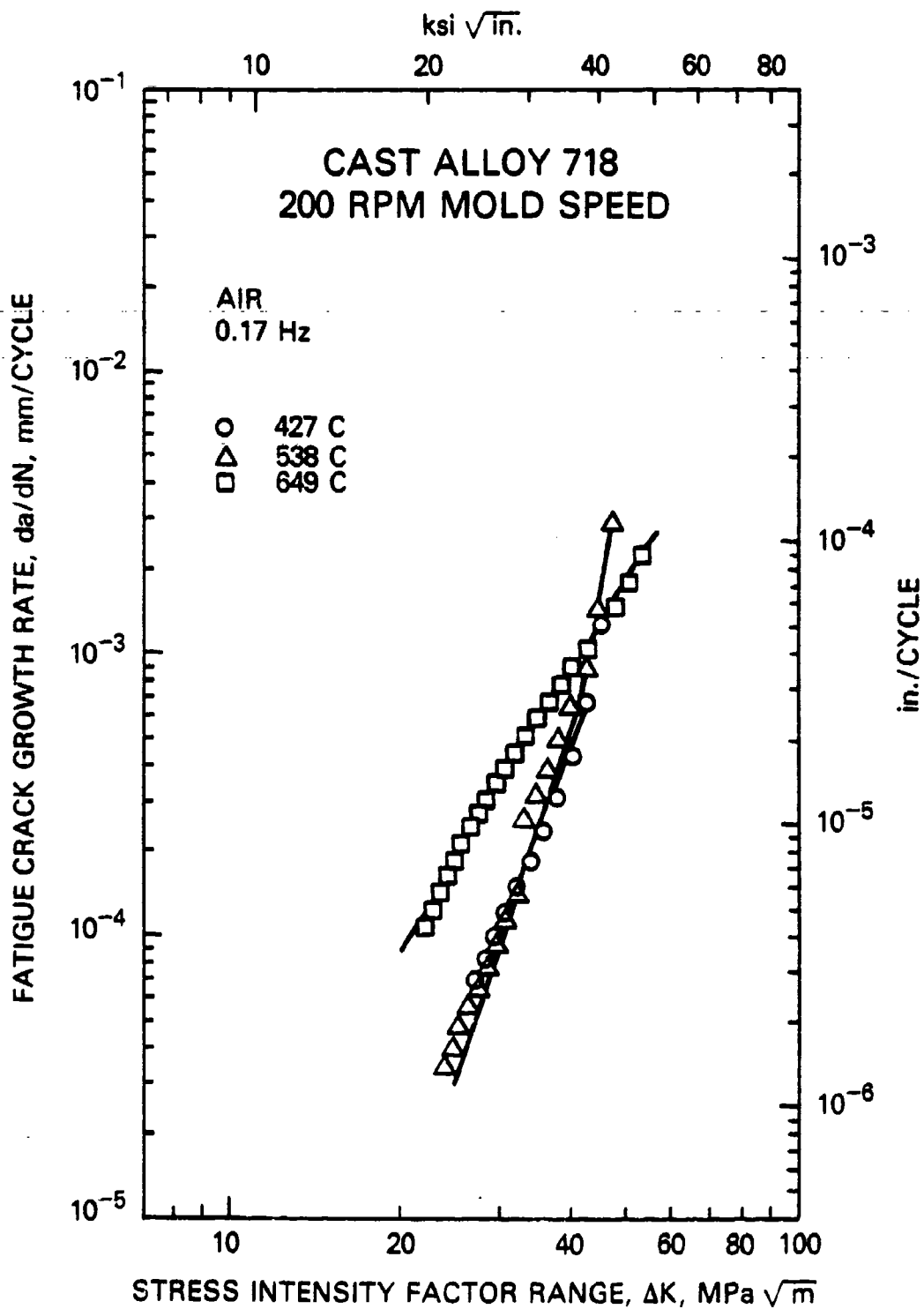


Fig. 6 Fatigue crack propagation performance of cast alloy 718 (200 rpm mold speed) in air at 0.17 Hz and at 427, 538 and 649°C. Notch orientation of the specimens was perpendicular to the cast disc radial direction.

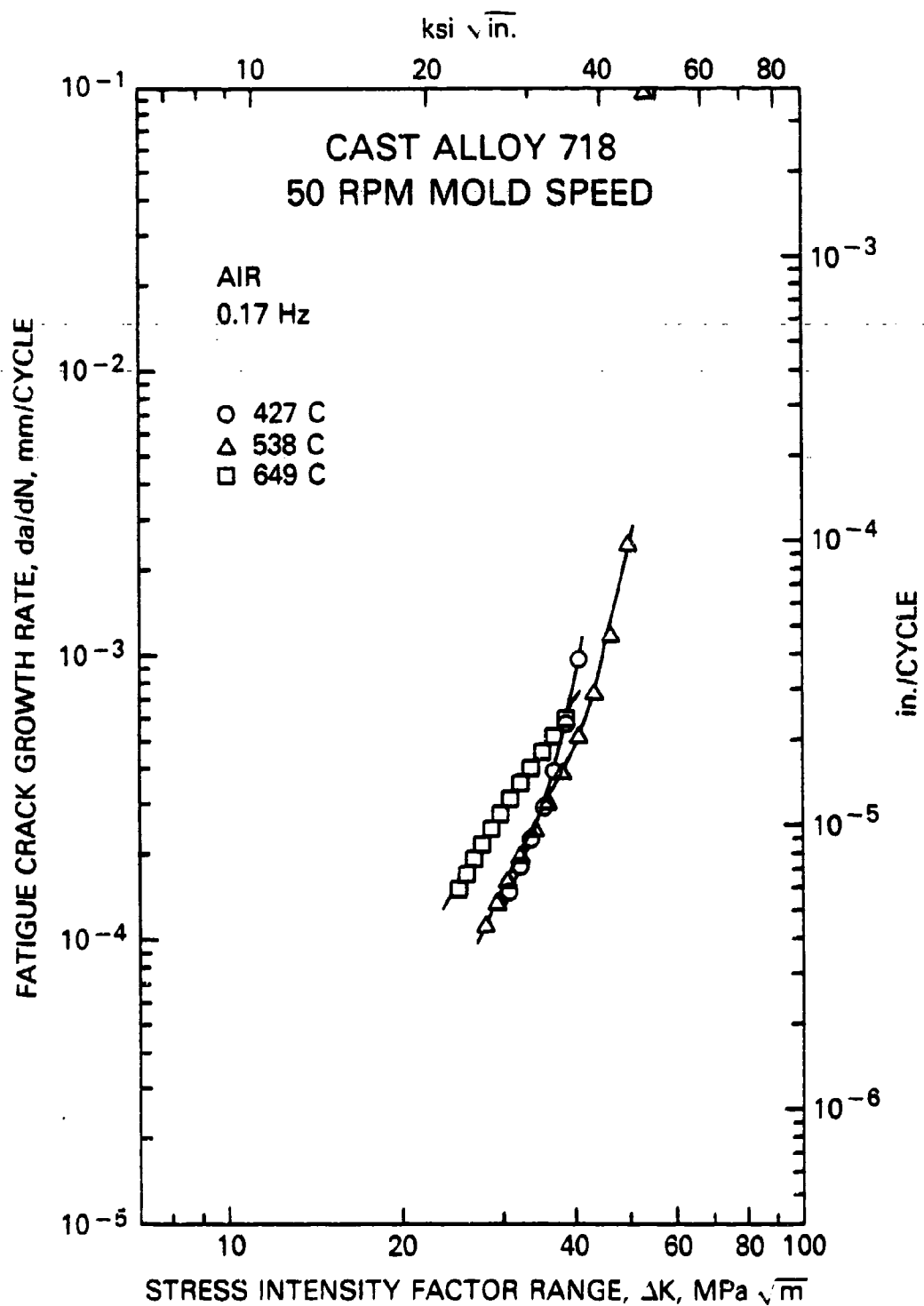


Fig. 7 Fatigue crack propagation performance of cast alloy 718 (50 rpm mold speed) in air at 0.17 Hz and at 427, 538 and 649°C. Notch orientation of the specimens was parallel to the cast disc radial direction.

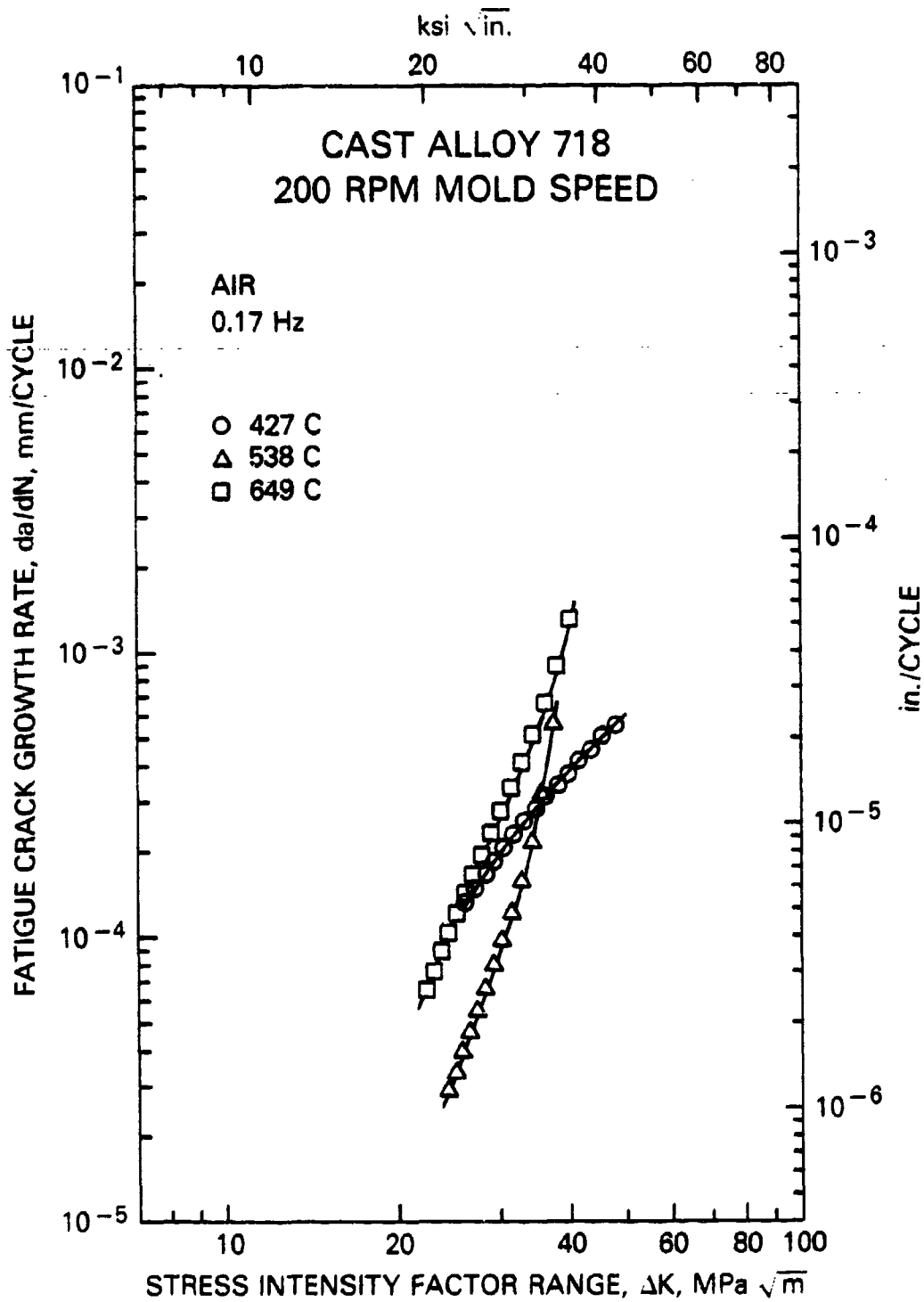


Fig. 8 Fatigue crack propagation performance of cast alloy 718 (200 rpm mold speed) in air at 0.17 Hz and at 427, 538 and 649°C. Notch orientation of the specimens was parallel to the cast disc radial direction.

TABLE 4
Composition (wt%) of Cast INCO 718
Determined by X-Ray Fluorescence Spectroscopy

Approximate Distance from Center of Casting, mm	50 rpm						200 rpm					
	Ti	Cr	Fe	Nb	Mo	Hardness Rc	Ti	Cr	Fe	Nb	Mo	Hardness Rc
46	.84	18.96	16.90	5.05	3.03	32	.89	18.54	16.94	5.40	3.26	33
61	.74	18.87	17.01	4.85	2.93	30	.83	19.30	17.13	5.10	3.11	31
76	.82	19.06	17.17	4.95	3.01	30	.77	18.65	16.96	4.96	3.03	31
91	.77	18.80	16.98	4.84	2.95	30	.78	19.11	17.09	4.87	3.01	30
107	.93	19.14	17.05	4.88	3.05	29	.78	19.29	17.04	4.93	3.06	29
122	.86	18.99	17.12	4.92	3.05	29	.70	19.09	17.29	4.83	3.00	30

primary constituents involved in the γ precipitates developed by the duplex age treatment. For a mold speed of 50 rpm, the compositional variation as a function of distance from the center of the casting shows no major discernable trends which would indicate elemental segregation as a result of the casting process. However, for a mold speed of 200 rpm the hardening elements were found to have an increased concentration towards the radial center of the casting. Hardness measurements of the same coupons verified that the hardness of the casting was slightly higher at the center as expected.

Figure 9 shows the through-thickness macrostructure of the cast disc. The dendrites, which grow from the cooled surface of the casting, have, in some instances, grown nearly halfway across the thickness. The grain size, taken as the size of a raft of parallel dendrites (same crystallographic orientation), varied widely. Unfortunately, because there was little microsegregation, a quantitative analysis of grain size was difficult. In general, the structure was more homogeneous than a static cast macrostructure and the results indicate that the centrifugal casting process has contributed to reduced microsegregation and increased homogeneity of structure and properties. In addition, there was no evidence of microporosity at either mold speed. At this magnification, the effect of speed on any grain refinement processes was uncertain. However, measurements at a magnification of 50x indicate a reduction in the primary and secondary dendrite arm spacings for the 200 rpm casting. The values of primary and secondary arm spacing were measured to be 233 and 86 μm and 195 and 70 μm for the 50 rpm and 200 rpm mold speeds, respectively. The effect of casting speed on carbide size and shape was significant as shown in Figure 10. At the 50 rpm speed, the carbides were large and elongated, Figure 10(a), as opposed to the rather symmetrically shaped and smaller carbides at 200 rpm, Figure 10(b).

Figure 11 shows the microstructure of the alloy 718 in the as-cast plus duplex age heat treatment condition for both mold speeds. Note the presence of a somewhat larger quantity of the second phase constituent in the alloy cast with the 50 rpm mold speed. Scanning electron microscope examination of the cast microstructure is shown in Figure 12 for the alloy cast at 200 rpm mold speed. The micrograph in Figure 12(a) shows the backscatter electron image of the dendritic character of the cast microstructure. Figure 12(b) shows the gamma (dark) matrix regions outlined by the precipitation of the Laves and carbide phases on the dendritic boundaries. Figure 12(c) shows the carbide phase (smaller particle) and the Laves phase (center of micrograph) present in the cast alloy 718 in the intermatrix areas. Note the composition shift of these phases as shown by the greatly increased niobium and titanium content of the carbide phase and the increase in niobium and molybdenum content of the Laves phase, relative to the matrix or bulk casting compositions.

For the low temperature duplex age employed in the present study, little Laves formation would be expected during heat treatment. During solidification, the Laves phase forms interdendritically in segregated areas impairing ductility and removing alloying elements required for precipitation hardening and, therefore, tends to reduce strength.

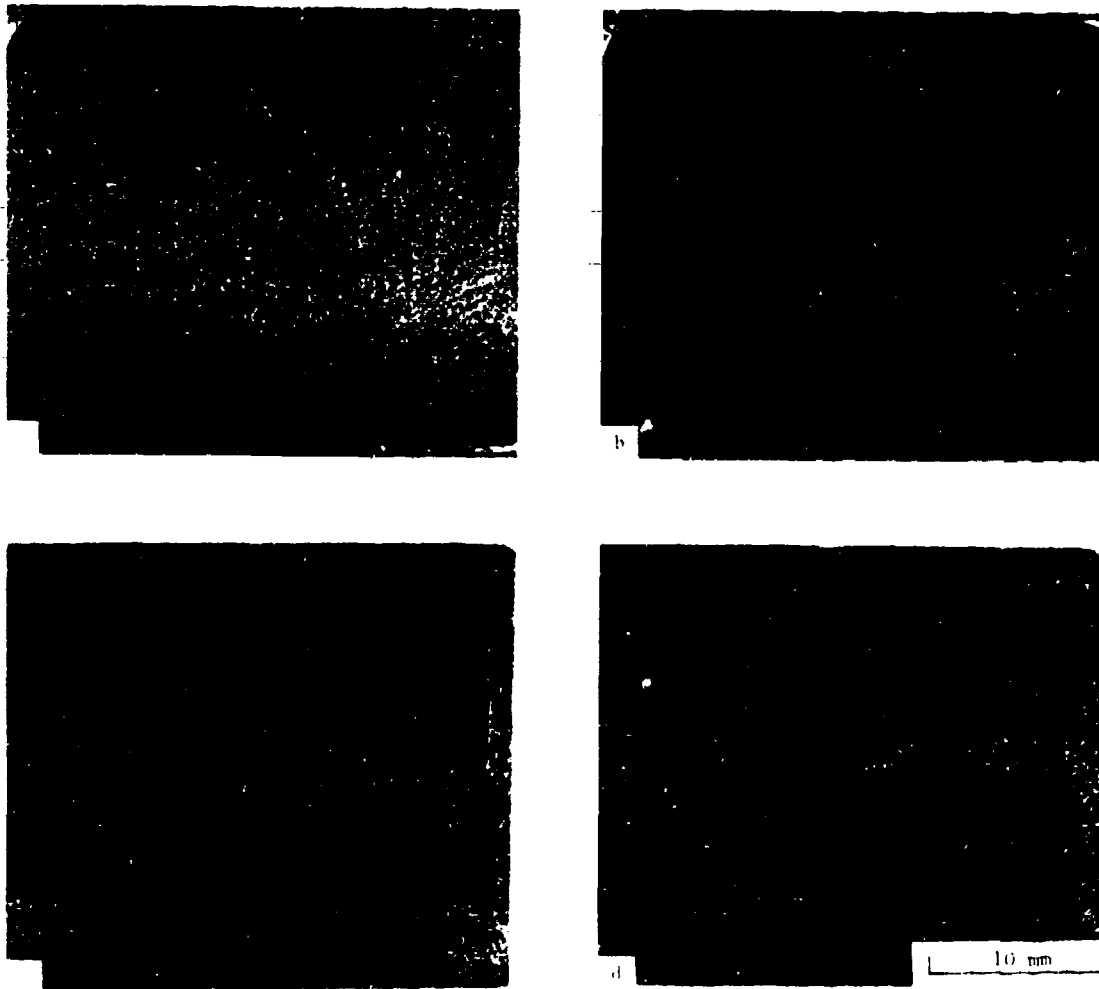


Fig. 9 Optical macrographs of the through-thickness microstructure of the centrifugally cast alloy 718: (a) radial and (b) transverse sections for 50 rpm mold speed; (c) radial and (d) transverse sections for 200 rpm mold speed.

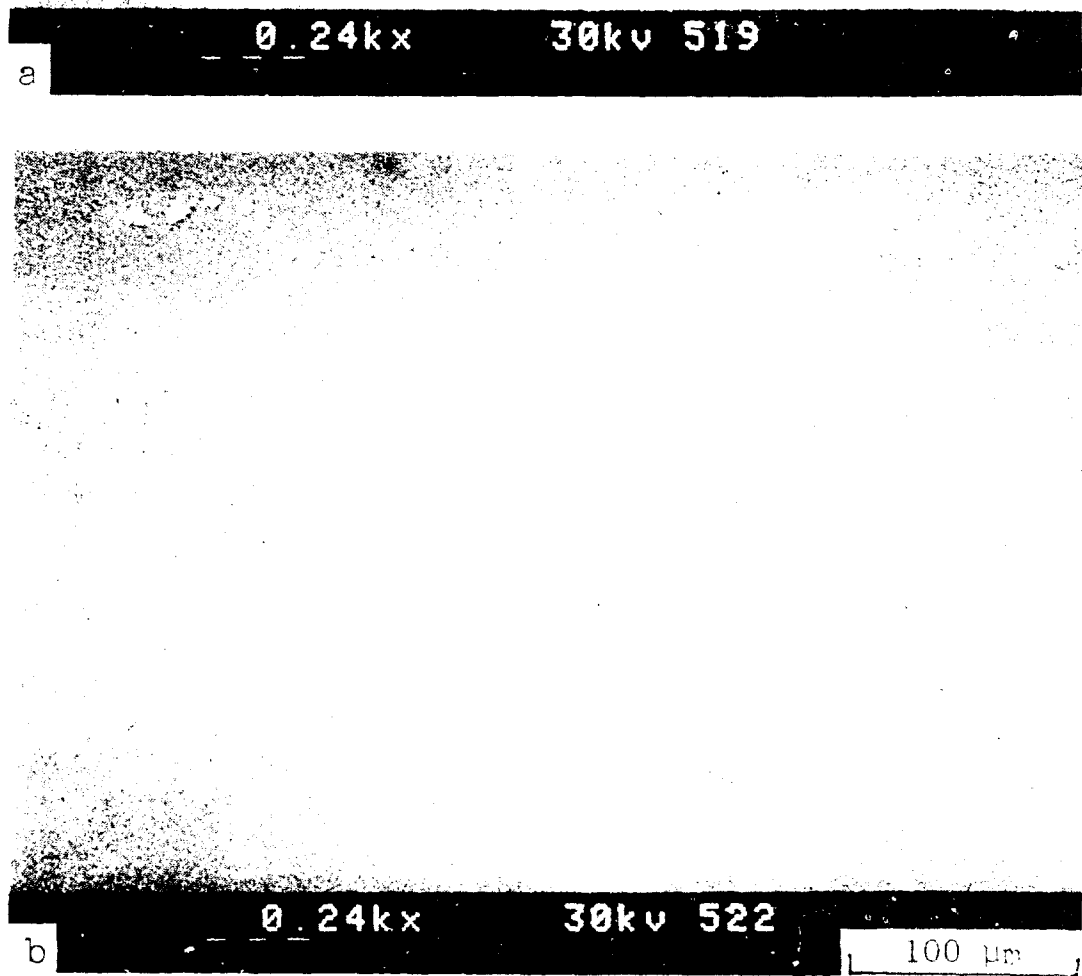


Fig. 10 Effect of casting speed on size and shape of carbide phase formation: (a) 50 rpm mold speed; (b) 200 rpm mold speed.

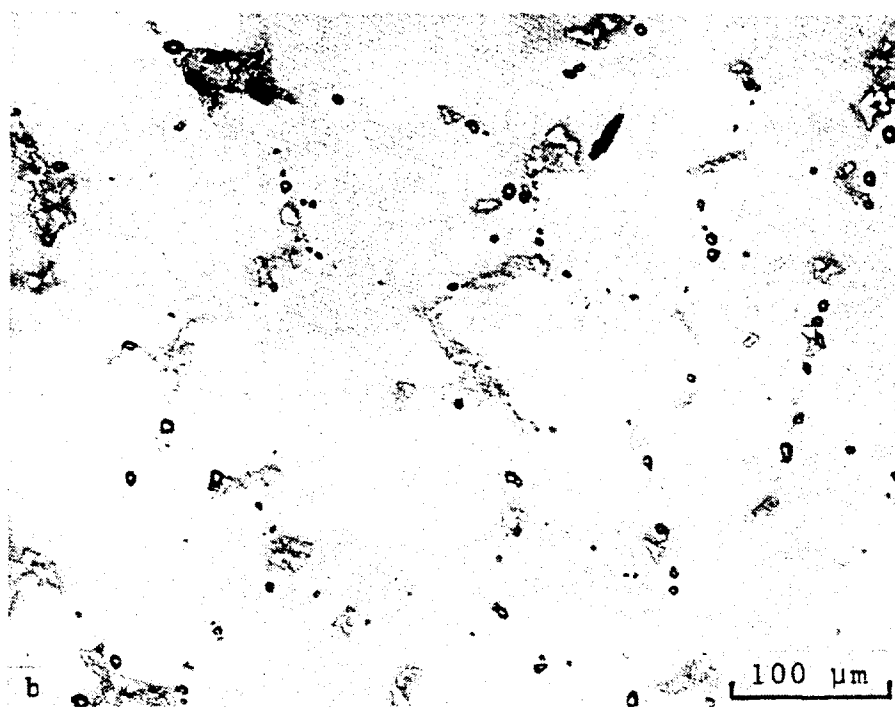
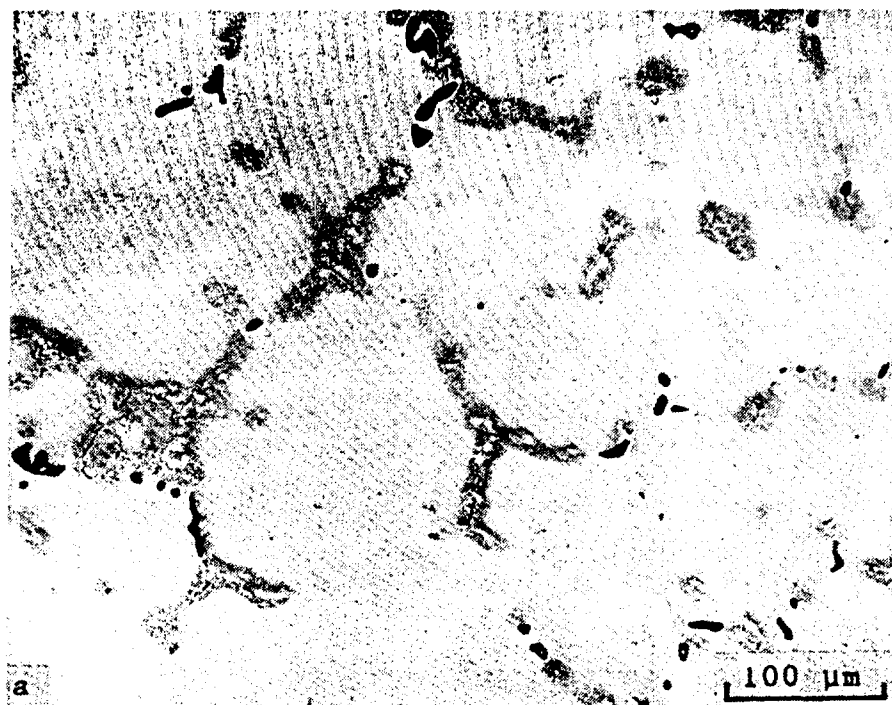


Fig. 11 Microstructure of centrifugally cast alloy 718 given the duplex age heat treatment; (a) 50 rpm mold speed; (b) 200 rpm mold speed.

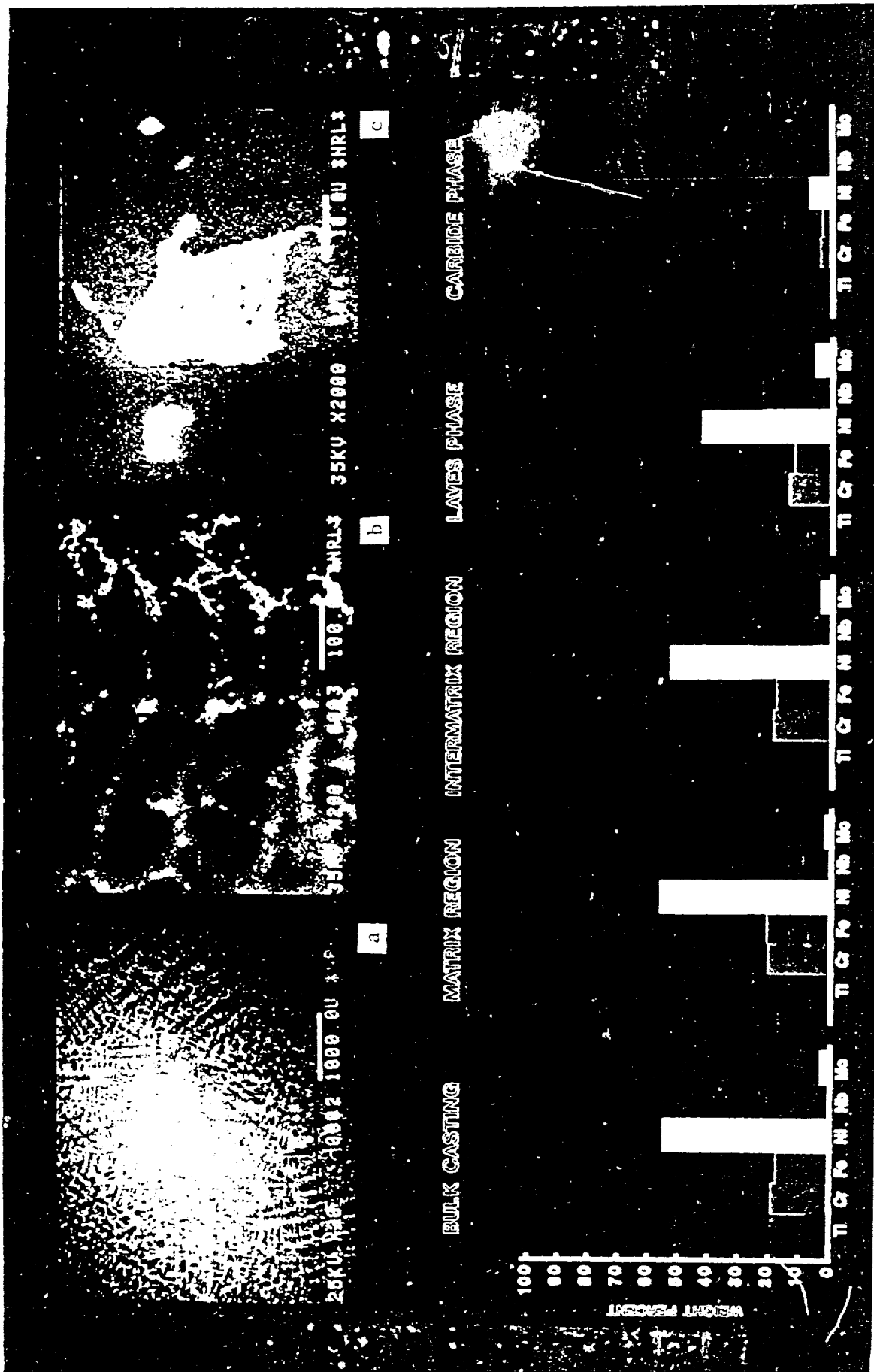


Fig. 12 Scanning electron micrographs of alloy 718 cast with the 200 rpm mold speed and the relative weight percentages of the alloy constituents; (a) backscatter electron image of the dendritic character; (b) dark gamma matrix outlined by laves and carbide phases; (c) carbide phase (small white particle) and laves phase (center of image) present in the intermatrix areas.

Fractographic Results

Scanning electron microscopy was used to investigate the mode of fracture for the tested tensile, creep-rupture and crack propagation specimens of the cast alloy 718. Figure 13 shows the fracture surfaces of the creep-rupture specimens tested to failure at 649°C. Note the limited capability of the cast microstructure for deformation by slip in both the radial and transverse directions and the evidence of the intermatrix-matrix region boundaries indicating that the fracture process is microstructurally sensitive. Figures 14(a) and 14(b) show sectional views of a fractured creep specimen. The specimen appears to have fractured along the interdendritic regions as shown in Figure 14(a) and Figure 14(b) shows evidence that the Laves phase is fracturing prior to the matrix. Figure 15 shows the influence of the cast microstructure on the fatigue crack propagation behavior. The fatigue crack initially propagated through the matrix areas, Figure 15(a). Note the highly crystallographic mode of crack growth which is predominantly cleavage. However, at higher levels of ΔK (above $\sim 24 \text{ MPa}\sqrt{\text{m}}$), the cracks tend to follow the intermatrix regions, Figure 15(b). Figures 15(c) and 15(d) show sectional views of the crack imaged with the secondary and backscatter electron modes, respectively, which illustrate a mixture of matrix and intermatrix crack propagation.

DISCUSSION

The results obtained in this study show that the centrifugal casting method, followed by a duplex age heat treatment, produced an alloy 718 microstructure whose creep and fatigue properties compared favorably with those of the wrought alloy. The centrifugal casting process was found to produce a microstructure free of porosity, but which exhibited segregation of the solute alloying elements to Laves and carbide phases, depending upon the mold speed used during casting. The microstructural results show that the predominant crack or fracture path was frequently associated with the carbide or Laves phases in the interdendritic regions. It is well known that alloy inhomogeneities are responsible for the reduction of the tensile and creep-rupture performance of materials at elevated temperatures.

Improvement of the properties of cast alloy 718 may be achieved by the reduction or elimination of alloy inhomogeneities in the as-cast microstructure. This may be accomplished through full solution heat treatment, either alone or in conjunction with mechanical working. The recently developed process known as hot isostatic pressing (HIP) serves to homogenize the alloy microstructure by re-solutioning the segregated alloying elements and the precipitate phases. When followed by a duplex age heat treatment, the homogenized microstructure will have improved tensile and creep-rupture properties, particularly at temperatures above 600°C (1110°F).

An example of the effectiveness of the HIP process to improve the microstructure is illustrated by comparing Figure 14(b) and Figure 16. In the backscatter electron micrographs of polished, unetched, cast alloy, the atomic number contrast has imaged the Laves phase a light gray and the carbides white. In Figure 14(b), which is before the HIP process, particle size analysis measurements indicated that the area fraction of Laves phase

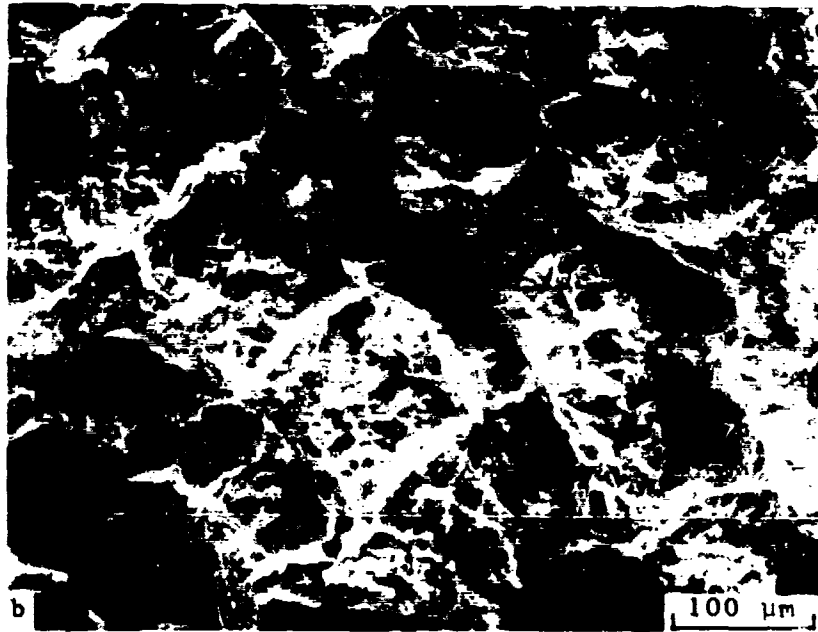
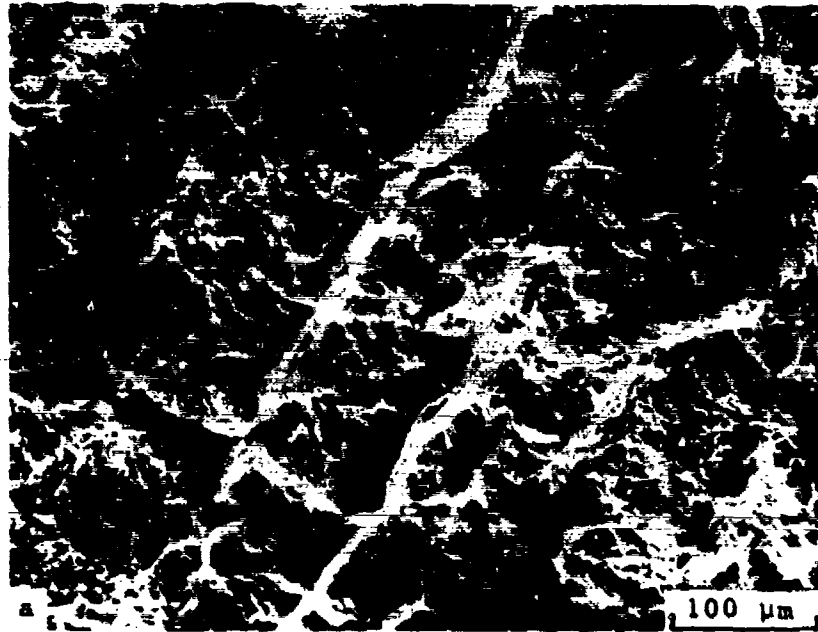


Fig. 13 Scanning electron micrographs of the fracture surfaces of cast alloy 718 creep-rupture specimens tested in air to failure at 649°C: (a) 50 rpm mold speed, specimen stress axis parallel to cast disc radial direction; (b) 50 rpm mold speed, specimen stress axis perpendicular to cast disc radial direction.

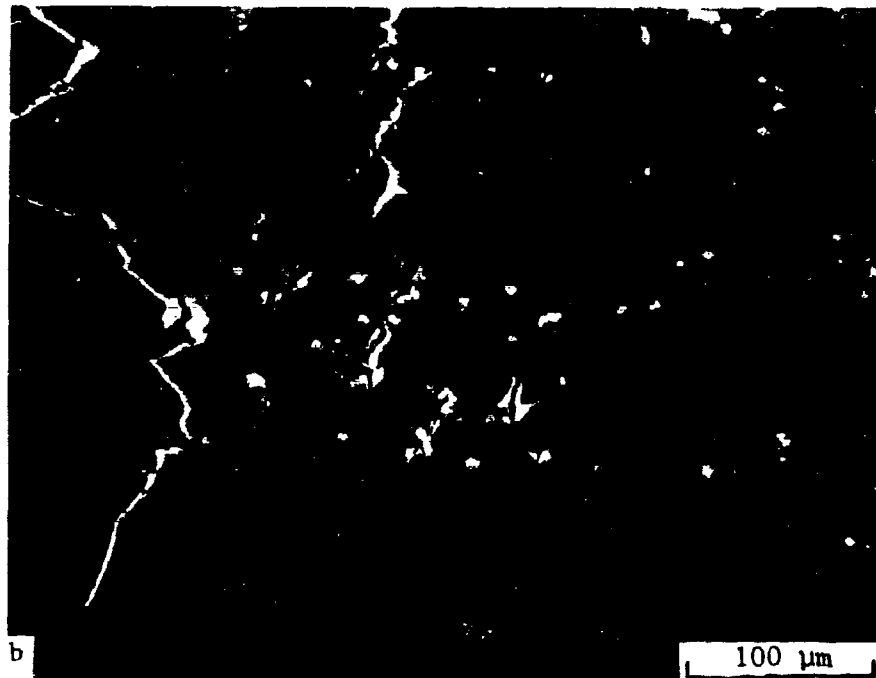
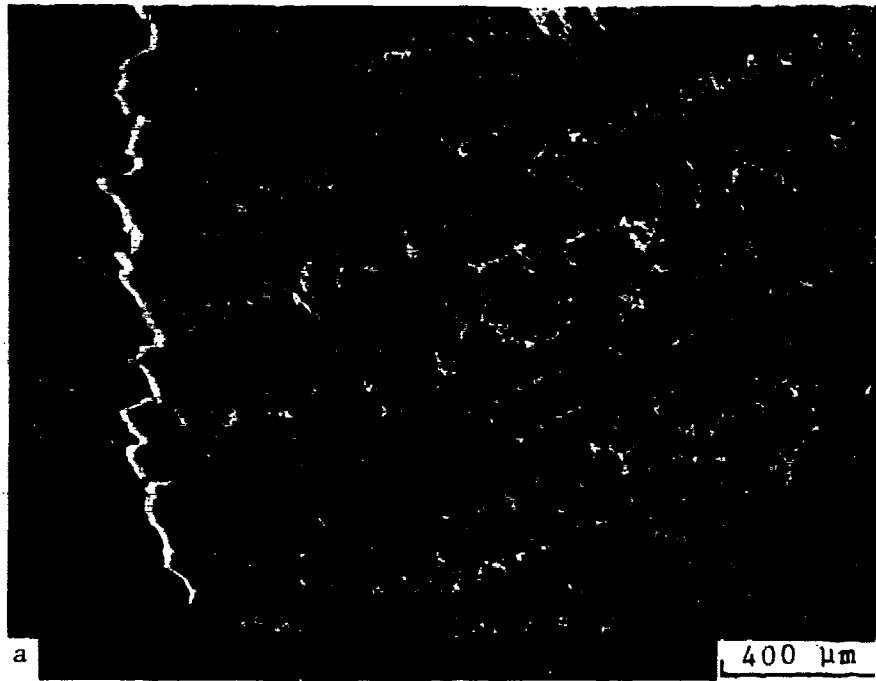


Fig. 14 Scanning electron micrographs (backscatter electrons) showing sectional views of a fractured creep specimen: (a) fracture follows interdendritic segregation; (b) evidence of Laves phase fracture prior to the matrix.

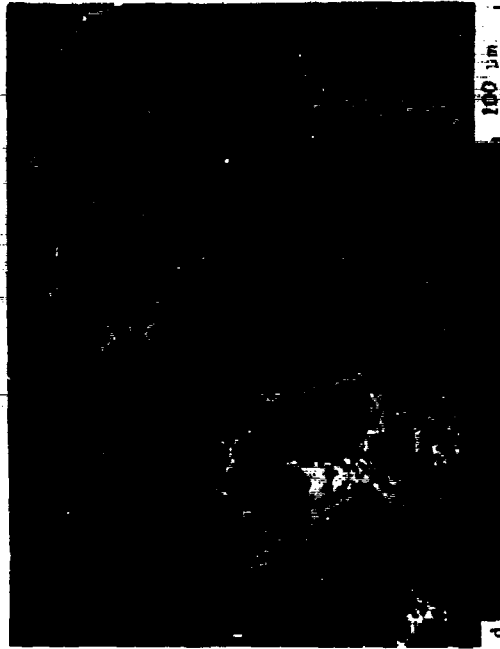


Fig. 15 Influence of cast alloy 718 microstructure on the fatigue crack propagation: (a) crack propagation through matrix by cleavage; (b) crack propagation through intermatrix regions at higher ΔK levels; (c) and (d) sectional views showing mixed matrix and intermatrix crack propagation.

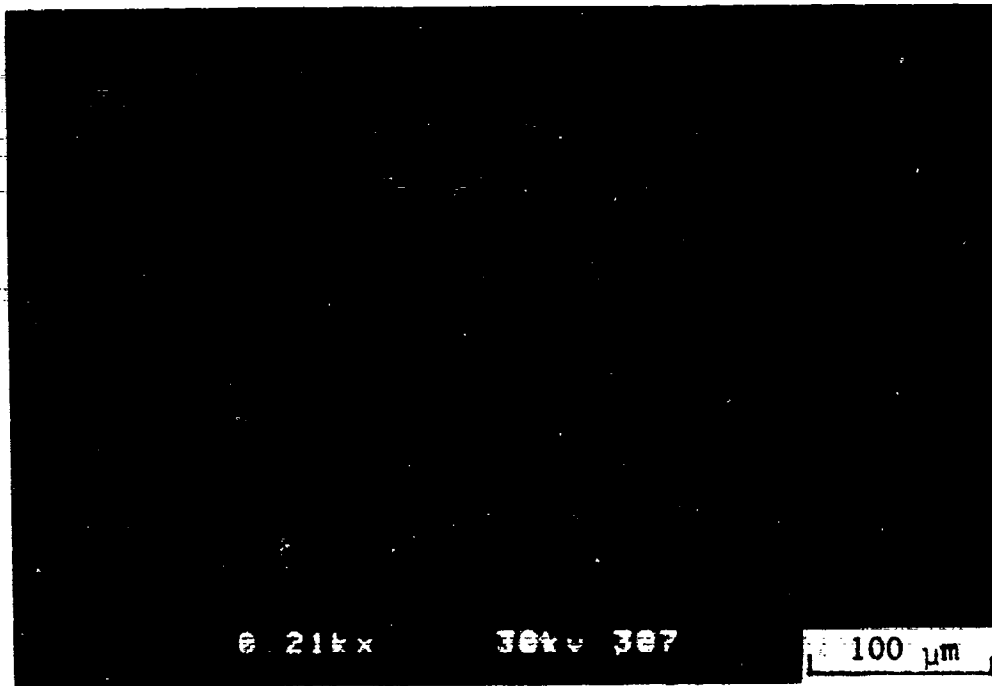


Fig. 16 Backscatter electron micrograph of cast alloy 718 following HIP treatment at 1200°C (prior to duplex age heat treatment).

is a minimum of three percent. Comparison of Figure 16 with Figure 16(b), which is after processing for four hours at 15 Ksi and 1200°C, shows that the interdendritic segregation and Laves structure has been effectively dissolved. It also appears that the carbide morphology has been altered while reducing the carbide population of the alloy. Although the alloy in Figure 16 has not received the duplex age heat treatment, the microstructural refinement provided by the HIP process points toward improved mechanical properties when compared with the as-cast microstructure.

A primary emphasis of this study was to evaluate the effectiveness of the centrifugal casting process to develop as-cast mechanical properties, which approach those of wrought product, in a near net shape configuration. Although the focus of the tests conducted was on the disc shapes, the results show that the higher mold speed produced both superior microstructural features, such as dendrite spacing and carbide phase shape, and creep-rupture life at 649°C. An improvement in the fatigue crack propagation behavior at 649°C also was noted for the higher mold speed. The results suggest that a further increase in mold speed may produce additional microstructural refinement and mechanical properties improvement. The upper limit to the potential improvement will depend upon the section thickness being cast. In order to examine the effects of section thickness and to study the properties of prototype castings, it is desirable to test actual component configurations, such as the compressor impeller, to determine the correspondence with the cast disc properties. The results of this evaluation, when coupled with the benefits of the HIP treatment will enable the program objectives to be achieved.

SUMMARY AND CONCLUSIONS

The tensile strength, creep-rupture life and fatigue crack propagation behavior of centrifugally cast alloy 718 were studied at temperatures from 427 to 649°C. The results reveal that the fatigue crack propagation properties of the cast alloy were similar to those of the wrought alloy when compared on the basis of the stress intensity factor range. Although the tensile strength of the cast alloy was less than for the wrought alloy, the creep-rupture properties of the cast alloy exceed those of the wrought alloy for creep loads determined on the basis of fraction of the tensile yield strength. The following conclusions are drawn from the results:

1. Centrifugally casting of alloy 718 produced no porosity for mold speeds of 50 and 200 rpm. However, the cast microstructure contained carbide and Laves phases, the latter as being generally regarded as deleterious to the mechanical properties of the alloy.
2. The tensile yield strength of cast alloy 718 was similar for specimens oriented either perpendicular or parallel to the cast radial direction.
3. The creep-rupture life was longest for material cast with the 200 rpm mold speed when tested at 649°C and at loads equal to 85% of the tensile yield strength. The larger strain at rupture was exhibited by specimens oriented such that the stress axis was transverse to the cast disc radial direction.

4. The fatigue crack propagation performance of the cast alloy 718 was similar to that for wrought alloy 718 at the stress intensity factor range levels studied and at the test temperatures of 427, 538 and 649°C.

5. The mode of crack propagation or rupture was found to follow the interdendritic segregation and the Laves and carbide phases preferentially at higher stress levels. A transition from the ductile crack path in the matrix to the intermatrix regions was observed with increased stress levels.

6. It is concluded that the use of HIP processing to reduce the solute segregation to the intermatrix regions, to the Laves phases and to the carbide phases, will improve the properties of the cast plus aged alloy 718.

ACKNOWLEDGMENTS

This research was supported by the Naval Material Command through the Naval Air Systems Command at the Naval Research Laboratory. The authors gratefully acknowledge the assistance and support of Mr. R. A. Retta, AIR-5143, and of Mr. C. E. Miller, formerly of AIR-5143, in the development of the research program on cast alloy 718.

REFERENCES

1. Standard Test Method of Tension Testing of Metallic Materials, ASTM Standard E8-82, 1983 Annual Book of ASTM Standards, American Society for Testing and Materials, Vol. 03.01, Metals - Mechanical Testing: Elevated and Low-Temperature Tests, pp. 119-139.
2. Standard Test Method for Constant-Load-Amplitude Fatigue Crack Growth Rates Above 10^{-8} m/Cycle, ASTM Standard E647-83, 1983 Annual Book of ASTM Standards, American Society for Testing and Materials, Vol. 03.01, Metals - Mechanical Testing: Elevated and Low-Temperature Tests, pp. 710-730.
3. D. J. Michel and H. H. Smith, "Effect of Neutron Irradiation on Fatigue and Creep-Fatigue Crack Propagation in Alloy 718 at 427°C," J. Nucl. Materials, (1984), to be published.
4. H. H. Smith and D. J. Michel, "Fatigue Crack Propagation and Deformation Mode in Alloy 718 at Elevated Temperatures," in Ductility and Toughness Considerations in Elevated Temperature Service, G. V. Smith, ed., MPC-8, American Society of Mechanical Engineers, New York, 1978, pp. 225-246.